Polymer Bulletin 30, 587–594 (1993)

Polymer Bulletin

Impact tests on filled and unfilled thermotropic liquid crystalline polymer injection mouldings

C. J. G. Plummer[1], Y. Wu[1,2], M. M. Gola[2], and H.-H. Kausch[1]

[1]Laboratoire de Polymères, Ecole Polytechnique Fédérale de Lausanne, CH-1015 Lausanne, Switzerland

[2]Dipartimento di Meccanica, Politecnico di Torino, Corso Duca degli Abruzzi 24, I-10129 Torino, Italy

Summary

Charpy and falling weight impact tests have been carried out on filled and unfilled thermotropic liquid crystalline mouldings between room temperature and 140 °C. There is progressive embrittlement on filler addition in both types of test, and a maximum in absorbed energy as a function of temperature is observed, corresponding to the glass transition temperature near 100 °C.

1. Introduction

The current investigation involves the Vectra™ 'A' series of filled and unfilled random copolyesters (Hoechst Celanese), whose composition is 73 %/27 % Hydroxybenzoic acid-Hydroxynaphthoic acid (HBA-HNA), with a glass-to-nematic transition, T_g, at approximately 100 °C. Vectra is a thermotropic liquid crystalline polymer (TLCP), characterized by rigid linear chains, which develop strong macroscopic alignment during flow. Since such alignment is substantially retained on solidification, TLCP injection mouldings often display exceptional mechanical properties in the flow direction, as well as extremely high levels of anisotropy and structural inhomogeneity, which are in turn critically dependent on the processing conditions. To avoid excessive anisotropy in unfilled TLCPs, the manufacturers generally recommend mineral or short glass fibre-filled grades for injection moulding. However, impact tests at room temperature show unfilled mouldings to display superior toughness to filled mouldings [1-3]. For example, the manufacturers give IZOD toughnesses of 520 and 70 Jm^{-1} respectively for unfilled Vectra A950 and 40 wt% wollastonite-filled Vectra A540 injection moulded bars tested in the flow direction [1] (that is, with the axis of flexion perpendicular to the flow direction). On the other hand, perpendicular to the flow direction, the high anisotropy of injection moulded TLCPs leads to a much lower IZOD toughness, and both the IZOD toughness and K_{Ic} *increase* on filler addition [2,3]. Given such contrasting behaviour, it is not clear how such tendencies should manifest themselves in other types of test, such as the biaxial falling weight test, whence the motivation for the present work.

The structure and basic mechanical properties of the Vectra mouldings investigated here are described in detail elsewhere [4,5]. They are typically characterized by the layered

structure shown schematically in Figure 1. The skin layers show relatively high molecular orientation in the flow direction. In the inner layers, however, the overall orientation is generally low, and in the inner core is often directed along parabolic 'flow lines' as sketched in Figure 1. Since it is more oriented, and hence stiffer, the skin carries a high proportion of the load at a given elongation. Hence, in spite of its relatively high tensile strength, failure of the skin (and consequent failure of the whole moulding) may occur at relatively modest overall loads. Indeed, the intrinsically weaker, but more uniform filled mouldings are often observed to have higher tensile strengths than the unfilled mouldings, depending on the relative proportions of skin and core, and hence on the moulding conditions and the sample geometry [4,5].

2. Experimental

Charpy impact tests were carried out using the CEAST instrumented pendulum. The specimens were injection moulded bars of Vectra A950 (unfilled) and Vectra A130 (30 wt% glass fibre filled) with 4 x 10 mm^2 rectangular cross-sections, whose static properties in the flow direction are given in Table I, supplied by B. Zülle of Asea Brown Boveri Ltd..

Material	Filler	Young's Modulus (GPa)	Tensile Strength (MPa)
A950	-	7.83	116.0
A130	30 wt% Glass fibre	17.65	187.5

Table I: Room temperature tensile properties of Charpy specimens (2 mm/minute)

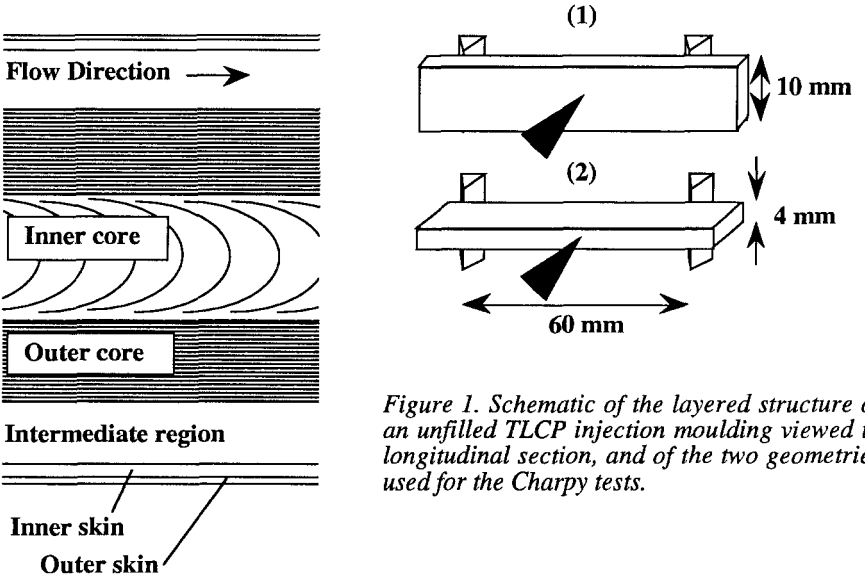

Figure 1. Schematic of the layered structure of an unfilled TLCP injection moulding viewed in longitudinal section, and of the two geometries used for the Charpy tests.

Tests were carried out in two geometries as sketched in Figure 1, using both un-notched and notched specimens. The notches were machined to the required depth, and a single pass with a fresh razor blade was used to induce a 'natural' crack at the notch tip. Tests at elevated temperature involved heating the sample to the required temperature, and then impacting it within 5 seconds of removal from the oven. The impact velocity was varied at a constant hammer mass of 1.095 kg with an arm length of 0.327 m.

The following standard method of analysis was used. The measured energy is

$$E_a = v_o \int_0^{tf} F dt \qquad \ldots (1),$$

where v_o is the initial velocity of the hammer, F is the measured force and t_f is the time elapsed after initial contact with the specimen. The true energy absorbed at t_f is

$$E = \int_0^{tf} F v dt \sim \bar{v} \int_0^{tf} F dt \qquad \ldots (2),$$

where $\bar{v}$ is taken to be $(v_o + v_f)/2$ where v_f is the hammer velocity at t_f. Since the integral in equation (1) gives the change in momentum of the hammer between t = 0 and t_f, then

$$\frac{\bar{v}}{v_o} = 1 - \frac{E_a}{4E_o} \qquad \ldots (3),$$

where $E_o = \frac{1}{2} m v_o^2$ is the energy available from the hammer. From (1) and (2),

$$E = E_a(1 - \frac{E_a}{4E_o}) \qquad \ldots (4).$$

An effective strain rate for a given test is given by

$$\frac{d\varepsilon}{dt} = \frac{6D\bar{v}}{S^2} \qquad \ldots (5)$$

for the three point bending geometry, where S is the distance between the supports, D is the thickness of the sample, and $\bar{v}$ is calculated at the point at which the force reaches its maximum F_{max}. For a sample width B, the corresponding stress maximum is given by

$$\sigma_{max} = \frac{3F_{max}S}{2BD^2} \qquad \ldots (6),$$

For such analysis to be valid, the tests should be substantially free from inertial disturbances. Problems tend particularly to arise at high striker speeds and in rubbery regimes of behaviour, where the period of oscillations in the force-time curves became comparable with the duration of the impact, preventing reliable measurement of F_{max}.

Biaxial falling weight impact tests were carried out on edge-gated 2 x 80 x 80 mm^3 injection moulded plaques supplied by H. Terwyen, Hoechst AG, Frankfurt am Main, using the CEAST Fractovis instrumented falling weight test apparatus with environmental chamber, and a hemispherical tup of mass of 3.01 kg. As well as A950 and A130, Vectra A515 (15 wt% mineral (wollastonite) filled) and Vectra A540 (40 wt% mineral filled) were investigated. The static properties of tensile bars cut from these plaques both perpendicular and parallel to the flow direction are listed in table II, giving an idea of the anisotropy. Comparison with table I illustrates the variation in properties with sample geometry and fabrication conditions.

Table II: Room temperature tensile properties of tensile bars cut from the falling weight impact specimens (2 mm/minute) with the tensile axis at 0 and at 90 °C to flow direction.

Material	Filler	Young's Modulus (GPa)	Tensile Strength (MPa)
A950 (0°)	-	12.0	140
A515 (0°)	15 wt% Wollastonite	9.4	145
A540 (0°)	40 wt% Wollastonite	13	140
A130 (0°)	30 wt% Glass fibre	10.0	147
A950 (90°)	-	3.0	50
A515 (90°)	15 wt% Wollastonite	3.2	50
A540 (90°)	40 wt% Wollastonite	6	50
A130 (90°)	30 wt% Glass fibre	6.8	64

3. Results

Charpy Tests. Figure 2 shows examples of the room temperature response of notched and un-notched A950 and A130, in geometry (1) of Figure 1. (Oscillations owing to discontinuous contact with the hammer are clearly visible.) In un-notched samples of A950, the maximum in the force displacement curve coincides with failure of the skin layer. Beyond this point, impact energy is absorbed by the propagation of L-shaped cracks along the fibrillar interfaces and ductile deformation of the inner part of the sample, this representing a substantial contribution to the total absorbed energy. The glass fibre-filled A130 mouldings show more brittle behaviour, that is, the force-displacement curve drops abruptly beyond its maximum and the total absorbed energy is essentially that required for crack initiation.

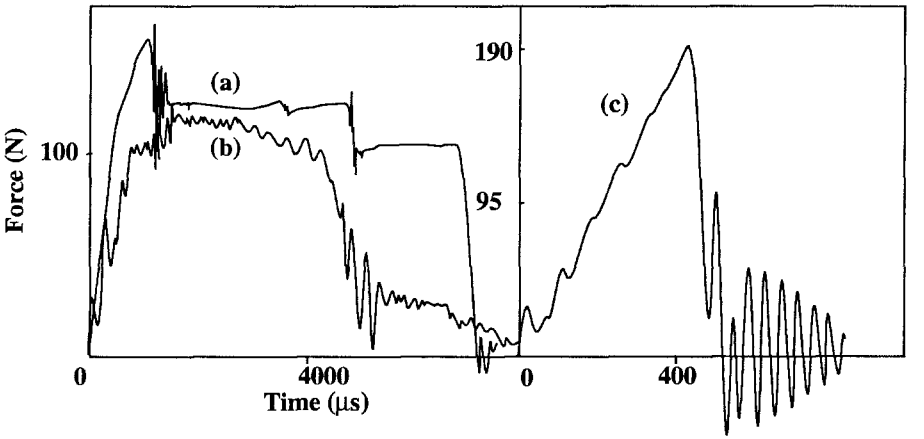

Figure 2. Force-time curves for Charpy tests in geometry (1) of Figure 1: (a) A950 un-notched; (b) A950 notched; (c) A130 un-notched.

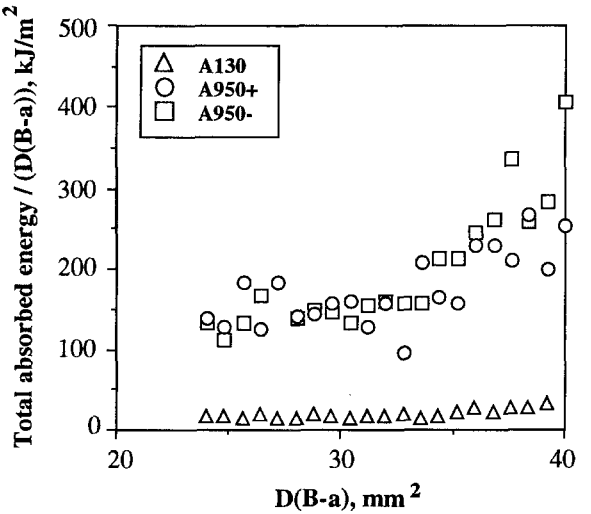

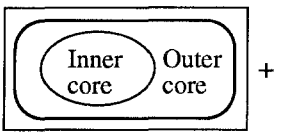

Figure 3. Total energy to rupture in Charpy tests in geometry (2) of Figure 1: a is the notch depth; A950+ refers to samples notched on the side furthest from the core and A950- to samples notched on the side closest to the core (see the above sketch of the sample cross-section).

The notched A950 sample of Figure 2 gives a more rounded force displacement curve with a lower force maximum than in the un-notched case, this corresponding to the effective absence of all or part of the skin layer. The effect of notching is shown more systematically in Figure 3 for geometry (2), where the total absorbed energy normalized with respect to the effective

cross-section is given as a function of the notch depth in both A950 and A130, at a striker energy of 15 J. Since the position of the inner core of the A950 samples was not exactly central (a side-gate having been employed to avoid jetting), the notches were introduced on either side of the samples with respect to the melt fill direction, as indicated in the Figure. In fact this made little difference; the main feature of the curves is an increase in the absorbed energy per unit area for notch depths less than approximately 0.5 mm. Optical examination and modulus profiles indicated this to represent the limit of the (symmetrical) outer core in these samples, whence the role of the outer layers is clear in raising the total absorbed energy. In the A130 samples a slight increase in total absorbed energy was also seen for notch depths less than 0.5 mm, but the behaviour remained brittle throughout. Hence whilst the absorbed energy per unit area in A950 ranged from approximately 150 to 300 kJm^{-2}, in A130 it did not exceed 25 kJm^{-2}.

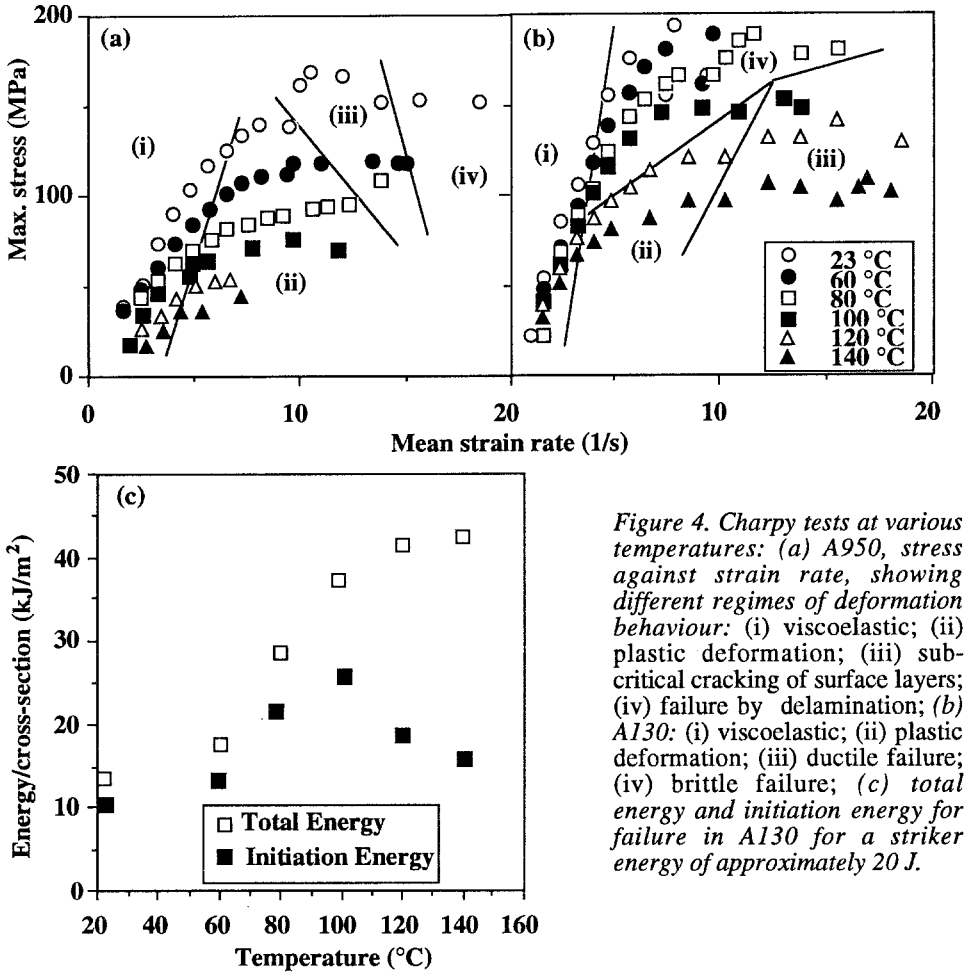

Figure 4. Charpy tests at various temperatures: (a) A950, stress against strain rate, showing different regimes of deformation behaviour: (i) viscoelastic; (ii) plastic deformation; (iii) sub-critical cracking of surface layers; (iv) failure by delamination; *(b) A130:* (i) viscoelastic; (ii) plastic deformation; (iii) ductile failure; (iv) brittle failure; *(c) total energy and initiation energy for failure in A130 for a striker energy of approximately 20 J.*

Above room temperature comparisons between A950 and A130 based on the failure energy become difficult with the present experimental set-up for the reasons given at the end of section 2. One can nevertheless gain some insight from changes in sub-critical deformation mechanisms with temperature, as shown in Figure 4, where the different regimes of behaviour

are related to the maximum stress and the effective strain rate for each test as calculated from equations (5) and (6) (this for the sake of illustration - it is beyond the scope of this communication to attempt a detailed analysis of these quantities).

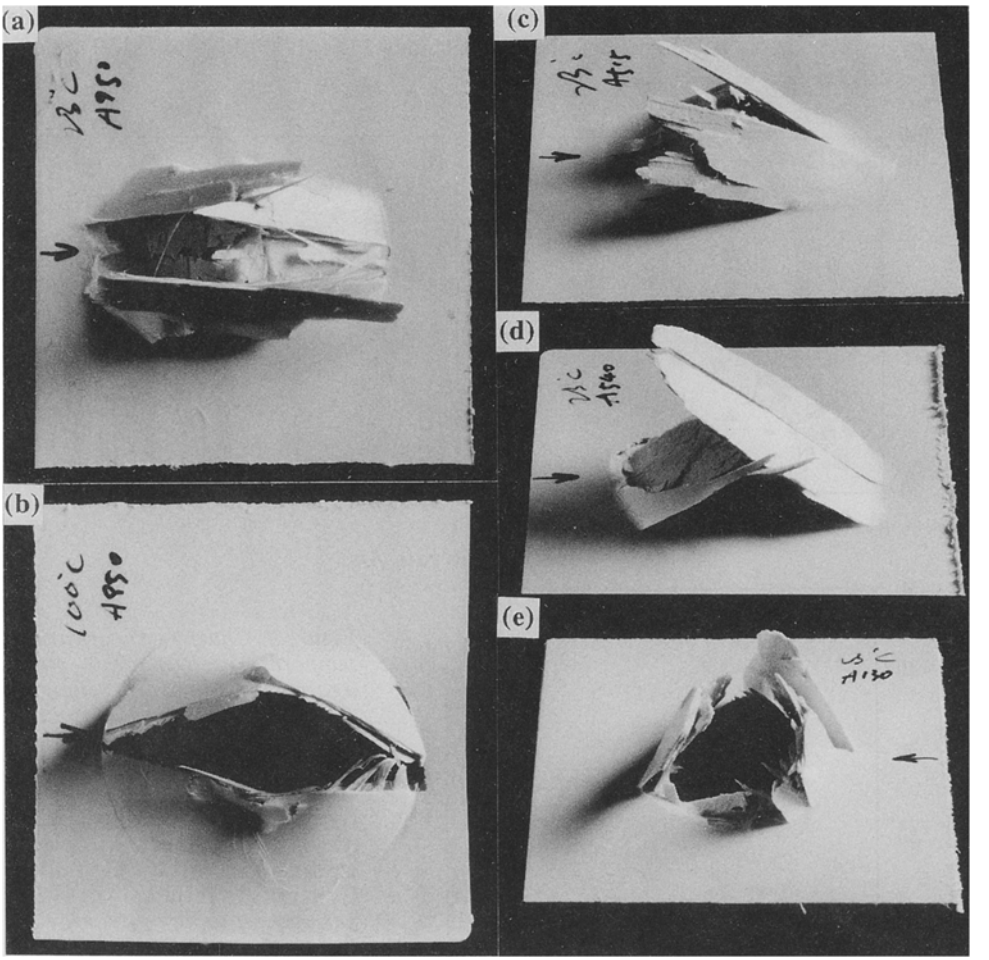

Figure 5. Falling weight impact tests on injection moulded plaques of Vectra: (a) A950, RT; (b) A950, 100 °C; (c) A515, RT; (d) A540, RT; (e) A130, RT (flow direction horizontal).

The low impact speeed response is viscoelastic (recoverable) deformation (characterized in both A950 and A130 by a parabolic increase with strain rate of the absorbed energy as the hammer rebounds). In A950 at room temperature, progressively higher strain rates lead initially to plastic deformation, followed by localized cracking in the skin and eventually to rupture by widespread delamination, whereas in A130, the onset of permanent deformation was marked by brittle fracture. As T increased, A950 became more ductile and the samples no longer ruptured in regimes accessible to the Charpy technique (Figure 4a). In A130, there was a transition from brittle to ductile fracture (Figure 4b), this latter characterized by widespread macroscopic plastic deformation on the fracture surfaces, and for T > 100 °C (T_g), permanent plastic deformation was observed without complete failure at intermediate strain rates. It was possible to obtain data for complete failure in A130 over the whole temperature range; there was a steep increase in the total energy for failure with temperature, and a peak in the energy for initiation of failure at approximately 100 °C (Figure 4c), consistent with the observation of a maximum in the elongation to fail with temperature in uniaxial tensile tests close to T_g [4]. The diverging behaviour of the total energy and the initiation energy at high temperature reflects the increasing role of damage propagation at the onset of macroscopically ductile behaviour.

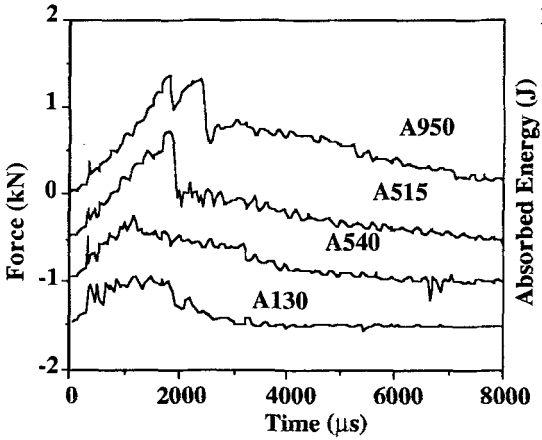

Figure 6. Force-time curves in room temperature falling weight impact tests at 4ms^{-1} on various grades of Vectra (zero of force displaced for clarity)

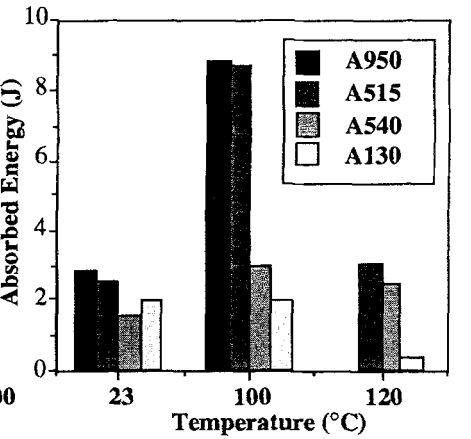

Figure 7. Total absorbed energy in falling weight impact tests at 4 ms^{-1} on various grades of Vectra.

Falling weight tests. The falling weight tests were also used to compare the different materials at elevated temperature. Figure 5 shows typical fracture surfaces, Figure 6 shows typical force-time curves and, finally, Figure 7 summarizes the measured values of the the total absorbed energy to failure. There was generally a maximum in total absorbed energy close to T_g at approximately 100 °C, its showing similar behaviour to the initiation energy for this type of test. In A950, the initial cracking in the skin layers at room temperature ran perpendicular to the flow direction, and was followed by considerable delamination (Figure 5a). One might imagine that in view of the high toughness anisotropy, the samples would tend to split along the flow direction. In fact this was the case when the temperature was raised (Figure 5b), possibly because the stiffness anisotropy tends to decrease towards T_g [4,5]. (A950 tested at temperatures higher than 100 °C did not undergo full rupture for the available range of impact speeds, although showing extensive plastic deformation.)

The absorbed energy decreased progressively with filler content as shown and the fracture surfaces become less anisotropic in appearance (Figure 5c - e), particularly on glass fibre addition, as reported by Wu *et al.* [6] for LCP 2000.

4. Conclusions

We believe the contrasting behaviours of unfilled and filled grades to be predominantly a result of modification of the matrix structure. The particle matrix interface in mineral filled grades fails well below the tensile strength and so plays no direct role in the ultimate properties. Glass fibres appear to show more effective bonding but even so there is a considerable drop in modulus just before failure in tension and the fracture surfaces show extensive fibre pullout as noted elsewhere [3]. It has also been noted that in notched fatigue tests that damage is very localized for glass fibre filled materials and there is no long range delamination [7], presumably because of the break-up of long range coherent structure in the presence of filler. This appears to be a key factor in the reduction of the impact resistance in the flow direction on addition of glass fibres and other types of filler. As discussed in the introduction, filler addition can improve the toughness perpendicular to the orientation direction in TLCP mouldings. Nevertheless, the biaxial falling weight tests showed similar qualitative behaviour to the Charpy tests, with again a progressive decrease in absorbed energy on mineral filler addition. Thus in general, it appears that if toughness is an important design consideration, the filler content should be kept to a minimum.

As T increased, both the unfilled and filled samples became more ductile, and a peak in the energy to failure initiation was seen for the Charpy tests on the glass fibre filled material close to T_g, consistent with the existence of a peak in the deformation to rupture in tensile tests. Similar peaks both in the energy to failure initiation and in the total absorbed energy were observed in the falling weight tests, with the glass fibre-filled material in particular showing very little impact resistance above T_g.

Acknowledgements

Financial support from the Swiss Commission pour l'Encouragement de la Recherche Scientifique (CERS) is gratefully acknowledged. Special thanks are due to H. Terwyen, Hoechst AG, Frankfurt am Main and B. Zülle of Asea Brown Boveri, Baden Dättwil for supplying certain of the specimens.

References

1. Vectra Technical Brochure, Hoechst-Celanese.
2. Chivers, R.A., Moore, D.R., Polymer 32, 2190 (1991).
3. Voss, H., Friedrich, K., J. Mat. Sci. 21, 2889 (1986).
4. Plummer, C.J.G., in "Advanced Thermoplastics and their Composites", Ch. 8, Kausch, H.-H. ed., Hanser, Münich.
5. Plummer, C.J.G., Wu, Y., Davies, P., Zülle, B., Demarmels, A., Kausch, H.-H., To be published in J. Appl. Poly. Sci..
6. Wu, J.S., Friedrich, K., Grosso, M., Compsites 20, 223 (1989).
7. Weng, T., Hiltner, A., Baer, E., J. Composite Materials 24, 103 (1990).

Accepted March 2, 1993 C